# LXRs regulate the balance between fat storage and oxidation

Nada Y. Kalaany,[1,8] Karine C. Gauthier,[1,7,8] Ann Marie Zavacki,[2] Pradeep P.A. Mammen,[3] Tatsuya Kitazume,[4] Julian A. Peterson,[4] Jay D. Horton,[3,5] Daniel J. Garry,[3,6] Antonio C. Bianco,[2] and David J. Mangelsdorf[1,*]

[1]Howard Hughes Medical Institute, Department of Pharmacology, University of Texas Southwestern Medical Center, 5323 Harry Hines Boulevard, Dallas, Texas 75390
[2]Division of Endocrinology, Diabetes, and Hypertension, Brigham and Women's Hospital, Harvard Medical School, 77 Avenue Louis Pasteur, Boston, Massachusetts 02115
[3]Department of Internal Medicine
[4]Department of Biochemistry
[5]Department of Molecular Genetics
[6]Department of Molecular Biology, University of Texas Southwestern Medical Center, 5323 Harry Hines Boulevard, Dallas, Texas 75390
[7]Present address: Laboratoire de Biologie Moléculaire et Cellulaire, UMR 5161-INRA LA 913, Ecole Normale Supérieure, 46 allée d'Italie, 69364 Lyon, France.
[8]These authors contributed equally to this work.
*Correspondence: davo.mango@utsouthwestern.edu

## Summary

**Despite the well-established role of liver X receptors (LXRs) in regulating cholesterol homeostasis, their contribution to lipid homeostasis remains unclear. Here we show that LXR null mice are defective in hepatic lipid metabolism and are resistant to obesity when challenged with a diet containing both high fat and cholesterol. This phenotype is dependent on the presence of dietary cholesterol and is accompanied by the aberrant production of thyroid hormone in liver. Interestingly, the inability of LXR$^{-/-}$ mice to induce SREBP-1c-dependent lipogenesis does not explain the LXR$^{-/-}$ phenotype, since SREBP-1c null mice are not obesity resistant. Instead, the LXR$^{-/-}$ response is due to abnormal energy dissipation resulting from uncoupled oxidative phosphorylation and ectopic expression of uncoupling proteins in muscle and white adipose. These studies suggest that, by selectively sensing the cholesterol component of a lipid-rich diet, LXRs govern the balance between storage and oxidation of dietary fat.**

## Introduction

The ability to store dietary fat and then utilize it as an energy source during times of privation is central to the survival of most animal species. An imbalance in this process can lead to serious health risks. As an example, obesity and its associated metabolic syndrome, characterized by onset of type II diabetes, hypertension, and heart disease, have reached epidemic levels in Western countries and are becoming increasingly prevalent worldwide (Grundy, 2004). Understanding the regulatory pathways that govern energy intake and storage (i.e., fat accumulation) versus energy expenditure (i.e., fat oxidation) is key to understanding diseases such as obesity. Recent efforts have begun to decipher the genetic as well as the environment-induced mechanisms underlying such an imbalance. Included in these studies has been the characterization of several transgenic mouse models that are resistant to diet-induced obesity. Most target genes identified in these studies fall into functional categories that either disturb normal adipocyte differentiation and lipid storage (*Pparg*, *Hmgi-c*), affect lipid synthesis (*Dgat*, *Complement c3*, *Scd-1*) or hydrolysis (*Perilipin*), increase fatty acid oxidation (*Acc2*, *Pgc1b*, *Ppard*) and energy uncoupling (*Ucp-1*, *Ucp-3*, *Cidea*), or modulate intracellular signaling in different tissues (*Pkariib*, *Ptp1b*, *Ikkb*, *S6k1*) (Chen and Farese, 2001; Ntambi et al., 2002; Kamei et al., 2003; Wang et al., 2003; Kopecky et al., 1995; Li et al., 2000; Clapham et al., 2000; Zhou et al., 2003; Yuan et al., 2001; Um et al., 2004).

The diversity of obesity-resistance genes leading to a common phenotype characterized by increased energy expenditure, enhanced glucose tolerance, and insulin sensitivity suggests the existence of a common set of factors that govern fat utilization (Chen and Farese, 2001). Candidate factors are likely to be upstream regulators capable of coordinating responses between different tissues and modifying the body's response to different lipid constituents of the diet. In this respect, members of the retinoid X receptor (RXR) heterodimer class of nuclear receptors are ideal candidates, since they bind to diet-derived lipophilic molecules and thereby modulate tissue-specific expression of downstream target genes involved in lipid homeostasis (Chawla et al., 2001). For example, the peroxisome proliferator-activated receptors (PPARα, PPARγ, and PPARδ) are activated by fatty acid derivatives, which in turn regulate gene networks that promote lipid synthesis and storage in adipocytes (PPARγ), or activate oxidation pathways in liver (PPARα) and muscle and brown adipocytes (PPARδ) (Evans et al., 2004). Likewise, the PPARγ coactivators PGC1α and PGC1β play essential roles in regulating energy metabolism in response to external stimuli by inducing fatty acid oxidation and hepatic gluconeogenesis (Puigserver and Spiegelman, 2003; Lin et al., 2002; Lin et al., 2003). The liver X receptors (LXRα and LXRβ) represent a second subset of lipid-sensing receptors that are well-known for their ability to sense oxysterols and regulate genes that decrease total body cholesterol levels (reviewed by Tontonoz and Mangelsdorf [2003]). LXRs are also potent stimulators of fatty acid and triglyceride synthesis. This effect is mediated in large part by LXR-dependent

hepatic expression of sterol regulatory element binding protein-1c (SREBP-1c) and its downstream targets, stearoyl-CoA desaturase-1 (SCD-1), acyl-CoA carboxylase (ACC), and fatty acid synthase (FAS) (Repa et al., 2000a; Yoshikawa et al., 2001). Pertinent to the present study, mice lacking SCD-1 and ACC-2 are resistant to obesity through increased lipid oxidation and energy expenditure (Ntambi et al., 2002; Abu-Elheiga et al., 2003). Taken together with the finding that cholesterol is often a component of a high-fat diet and shares common metabolic pathways with lipids, we explored the possibility that LXR regulation of lipid metabolism is interdependent on its ability to maintain cholesterol homeostasis.

In this study, we show that LXR null mice are defective in hepatic lipid metabolism and resistant to obesity when challenged with a Western-style diet containing both high fat and cholesterol. This phenotype is dependent on the presence of dietary cholesterol and is accompanied by the abnormal oxidation of fat in peripheral tissues. Importantly, this phenotype is independent of SREBP-1c, which is known to govern diet-induced hepatic lipogenesis and is a well-known target gene of the LXRs. Instead, we show that at least part of the mechanism driving the LXR$^{-/-}$ response may be due to abnormal, cholesterol-dependent production of thyroid hormone in liver and to the net increase in the energy utilization in muscle and white adipose. Altogether, these studies suggest a dual role for LXRs, which, by limiting accumulation of diet-derived cholesterol, permit the normal uptake and storage of dietary fat, a crucial element of a mammal's ability to efficiently utilize an important source of dietary fuel.

## Results

### Resistance to diet-induced obesity in LXR$^{-/-}$ mice requires dietary cholesterol

To study the role of LXRs in dietary fat metabolism, wild-type and LXR$\alpha$/LXR$\beta$ double-knockout (LXR$^{-/-}$) mice were maintained for 7 weeks on one of three diets: a standard rodent chow diet (4% fat; $\leq$0.04% cholesterol), a Western diet containing high fat and high cholesterol (21% milk fat, 0.2% cholesterol), or a high-fat-only diet, which has the same components as the Western diet but with no added cholesterol (21% milk fat; $\leq$0.05% cholesterol). As expected, wild-type mice gained weight significantly (up to 30% increase) when fed either of the high-fat diets compared to the standard chow diet (Figures 1A and 1B). In contrast, LXR$^{-/-}$ mice were 15%–20% leaner than their wild-type littermates at the beginning of the experiment and were resistant to weight gain when fed the Western diet (Figure 1A). Surprisingly, when the LXR$^{-/-}$ mice were maintained on the same diet without added cholesterol (i.e., the high-fat-only diet), they gained weight at the same rate and to the same extent as wild-type controls (Figure 1B). These same mice were also subjected to nuclear magnetic resonance (NMR) spectrometry to measure total body lipids on all three diets. NMR analysis showed that the observed changes in body weights in wild-type mice on a Western or high-fat-only diet and LXR$^{-/-}$ mice fed the high-fat-only diet were due to a 3-fold increase in body fat after 7 weeks of feeding (data not shown).

To examine whether obesity resistance in LXR$^{-/-}$ mice was due to alterations in feeding behavior, caloric intake and fat absorption were also measured. Despite their inability to gain weight on Western diet, LXR$^{-/-}$ mice exhibited a caloric intake per lean body mass that was comparable to that of wild-type mice fed the same diet (Figure 1C). When integrated into a formula that takes into consideration food intake, stool output, and lipid content, no significant changes in fat absorption were observed in LXR$^{-/-}$ mice compared to wild-type mice on Western diet (Figure 1D). These results revealed that LXR$^{-/-}$ mice are unable to store dietary fat in spite of normal food intake and absorption, and, thus, they are resistant to diet-induced obesity. Furthermore, this resistance required the inclusion of cholesterol as a component of the lipid-enriched diet.

### Protection from hyperlipidemia and insulin resistance in LXR$^{-/-}$ mice

To further characterize the obesity resistant phenotype in LXR$^{-/-}$ mice fed a high-fat/high-cholesterol diet, lipid and carbohydrate metabolism were analyzed. As expected from previous work (Peet et al., 1998), LXR$^{-/-}$ mice accumulated significantly more hepatic cholesterol compared to wild-type littermates when maintained on the Western diet (Figure 2A). Total plasma cholesterol was elevated in both wild-type and LXR$^{-/-}$ mice fed the Western diet, albeit to a lesser extent in LXR$^{-/-}$ mice (Figure 2B). Lipoprotein analysis revealed that, in wild-type animals, this increase in plasma cholesterol was all in the HDL fraction, while, in the LXR$^{-/-}$ mice, only the LDL/IDL fraction increased (Figure 2C). These findings are consistent with the notion that LXRs are required for governing reverse cholesterol transport by elevating HDL cholesterol and increasing hepatic cholesterol catabolism and excretion (Repa and Mangelsdorf, 2002).

In contrast to cholesterol, triglyceride metabolism was altered diametrically in LXR$^{-/-}$ animals. The Western diet increased hepatic triglycerides 8-fold in wild-type mice as expected, but no significant increase was observed in LXR$^{-/-}$ mice (Figure 2D). LXR$^{-/-}$ mice also maintained markedly lower plasma triglycerides and free fatty acids independent of diet, while both of these lipid pools increased significantly in wild-type mice on the Western diet (Figures 2E and 2G). Lipoprotein analysis revealed that LXR$^{-/-}$ animals had substantially lower triglycerides in their VLDL fraction on a chow diet, and this level was reduced further upon feeding the Western diet (Figure 2F). This result is consistent with the finding that hepatic fatty acid synthesis rates were markedly suppressed (60%–80%) in LXR$^{-/-}$ mice fed either chow or Western diet (Figure 2H) and supports the notion that dietary lipids were cleared from plasma by uptake and utilization in the periphery (see below). As an indicator of body fat and insulin resistance, and consistent with their obesity and hyperlipidemia, leptin and insulin levels in wild-type mice increased substantially (6-fold) on the Western diet compared to standard chow (Figures 2I and 2J). In comparison, basal levels of both plasma leptin and insulin were lower in LXR$^{-/-}$ mice and did not increase significantly when challenged with the Western diet (Figures 2I and 2J). Moreover, when injected with D-glucose, LXR$^{-/-}$ mice, which had lower fasting plasma glucose levels than wild-type mice, maintained significantly lower blood glucose levels at all assayed time points (Figure 2K). Consistent with their similar gains in weight, wild-type and LXR$^{-/-}$ mice fed the high-fat-only diet showed high levels of plasma insulin and leptin levels that were comparable to wild-type mice fed a Western diet (data not shown). Together, these results provide further evidence that the presence of dietary cholesterol plays an impor-

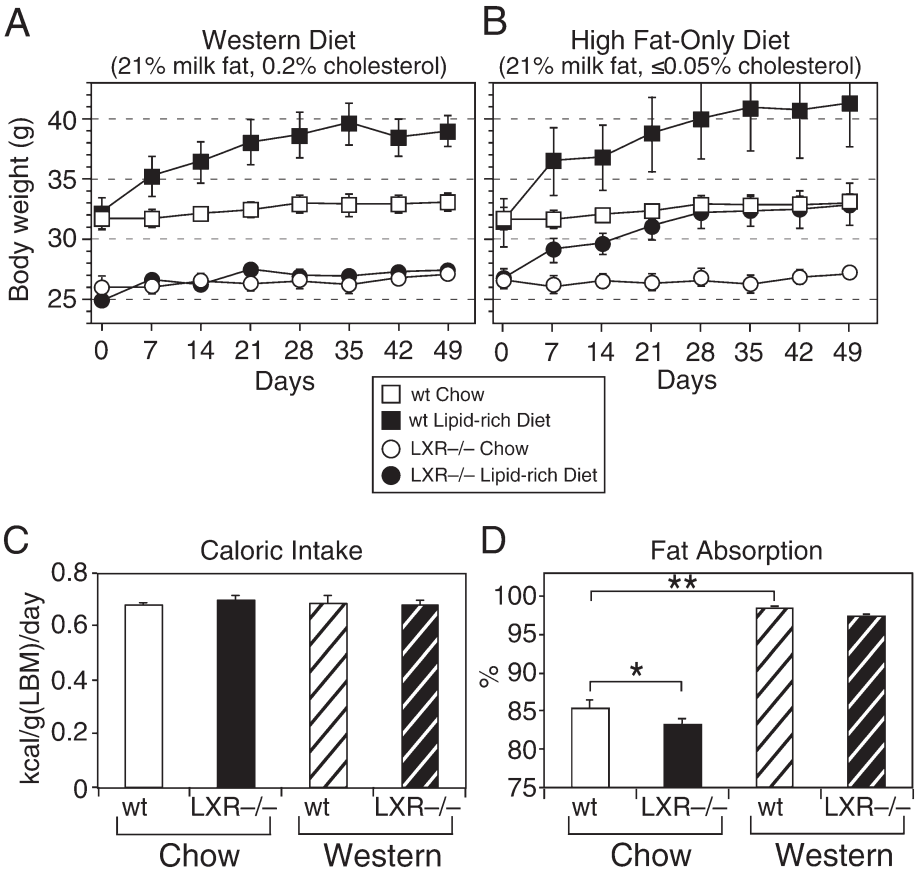


**Figure 1**. Cholesterol-dependent resistance to diet-induced obesity in LXR$^{-/-}$ mice

**A and B)** Growth curves of wild-type and LXR$^{-/-}$ mice (n = 5) fed chow versus Western diet (**A**) or chow versus high-fat-only diet (**B**).

**C)** Caloric intake of wild-type and LXR$^{-/-}$ mice (n = 6) after 7 weeks of feeding. Caloric intake (kcal/g lean body mass [LBM]/day) = food intake (g diet/g LBM/day) × caloric value of diet (kcal/g). Note that chow diet has 3.23 kcal/g; lipid-rich diets have 4.53 kcal/g.

**D)** Fat absorption of wild-type and LXR$^{-/-}$ mice (n = 5) measured on week 5 of feeding. Fat absorption = ([food intake × food lipid content] – [stool output × stool lipid content])/(food intake × food lipid content) × 100. *$p < 0.05$, **$p < 0.01$.

tant role in protecting LXR$^{-/-}$ mice from the effects of diet-induced hyperlipidemia.

### Altered expression of genes involved in hepatic lipid metabolism in LXR$^{-/-}$ mice

To address the mechanism by which LXR$^{-/-}$ mice metabolize dietary fat, we performed a real-time, quantitative PCR (QPCR) analysis of genes involved in the regulation of lipid metabolism in four tissues known to play a major role in this regulation, namely liver, muscle, and white and brown adipose tissues (Figures 3 and 5; see Figure S1 in the Supplemental Data available with this article online). Expression data were collected from both wild-type and LXR$^{-/-}$ mice fed either standard chow or high-fat diets for 7 weeks. In liver, marked changes were seen in the expression of genes involved in cholesterol, lipid, and carbohydrate metabolism, supporting previous work from our laboratory and others showing liver to be a major target organ of LXR (reviewed in Tontonoz and Mangelsdorf [2003]). As expected, LXR target genes involved in elimination of dietary cholesterol by catabolism (*Cyp7a1*) and biliary excretion (*Abcg5*, *Abcg8*) were not regulated in LXR$^{-/-}$ mice as in wild-type mice; similar data were observed for genes governing glucose metabolism (Figure S1A). Expression of genes involved in β oxidation of fatty acids (e.g., carnitine palmitoyltransferase-1a, *Cpt-1a*; acyl-CoA oxidase, *Aco*; very long chain acyl-CoA dehydrogenase; *Vlcad*) were not affected by the loss of LXRs, and coincidently, expression of genes in the PPARα metabolic cascade remained relatively unchanged or were decreased in LXR$^{-/-}$ mice (Figure S1A). However, in concordance with their altered hepatic lipid metabolism, expression of virtually every gene involved in fatty acid and triglyceride synthesis was decreased below basal levels in LXR$^{-/-}$ animals (e.g., *Fas*, *Acc1*, *Scd-1*, *Spot14*, malic enzyme [*Me*]) (Figure 3A; Figure S1A). In particular, expression of *Srebp-1c*, which encodes the transcriptional regulator of the genes in this pathway, was reduced to well below basal levels in LXR$^{-/-}$ animals under all dietary conditions, supporting the conclusion that LXRs are crucial for both basal and diet-inducible expression of hepatic SREBP-1c.

To test whether the resistance to obesity in LXR$^{-/-}$ mice was due to the loss of the SREBP-1c lipogenic pathway, SREBP-1c$^{-/-}$ mice were subjected to the same dietary analysis described above for LXR$^{-/-}$ and wild-type mice. Despite their smaller body weight at the beginning of the experiment, SREBP-1c$^{-/-}$ mice were not protected against diet-induced obesity and, like their wild-type littermates, gained significantly more weight (25%) when fed a Western versus standard chow diet (Figure 4A). NMR measurements of total body lipids revealed a 150%–200% increase in body fat over body weight (BF/BW) ratio in SREBP-1c$^{-/-}$ mice similar to the one observed in wild-type mice (Figure 4B). Consistent with their increased weight gain and in contrast to LXR$^{-/-}$ mice, SREBP-1c$^{-/-}$ mice had increased triglyceride levels in liver, but not in plasma, and increased plasma free fatty acids, insulin, and leptin levels in response to Western diet feeding (Figures 4C–4G). In addition,

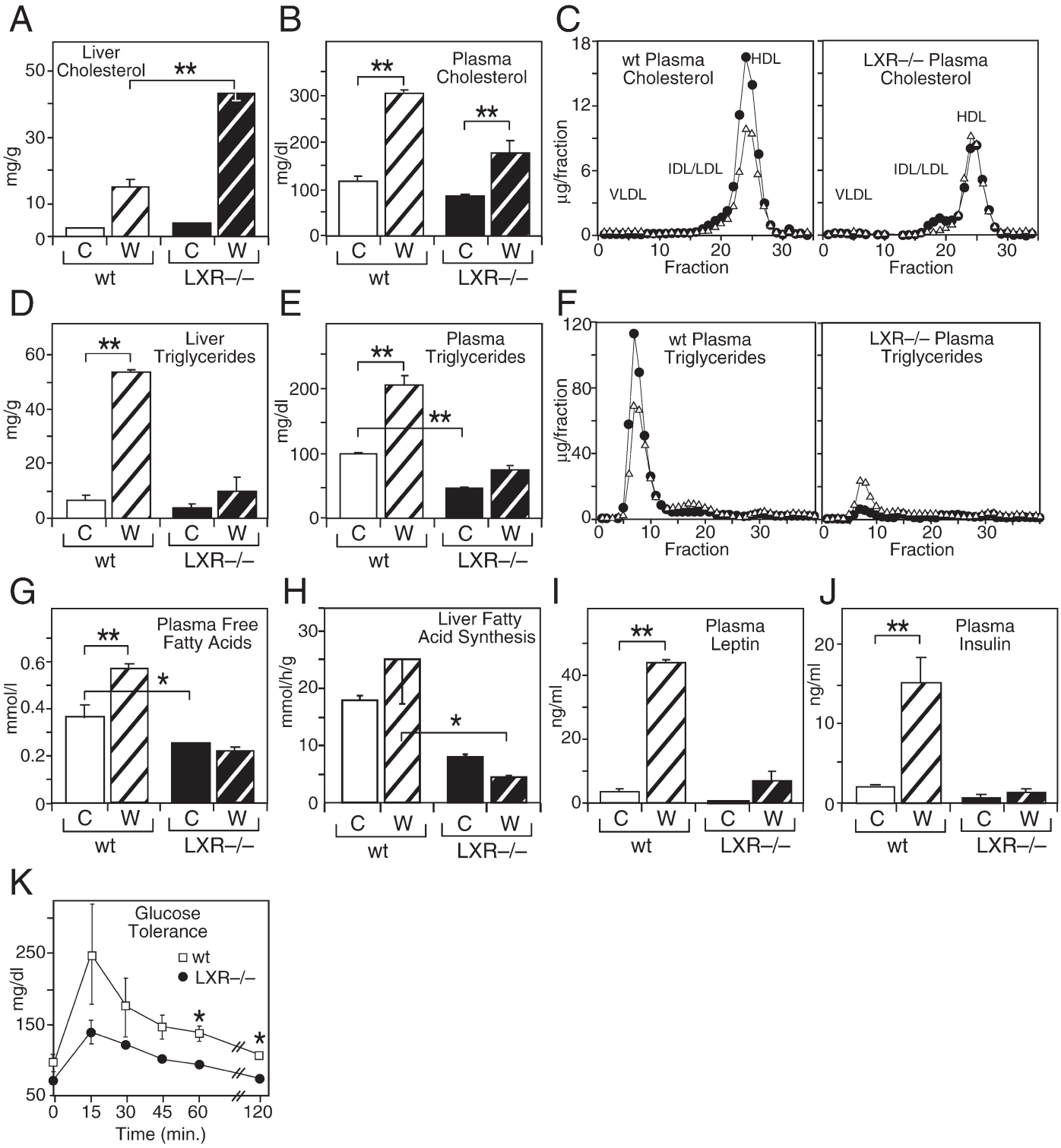


**Figure 2**. Liver and plasma lipid metabolism in wild-type and LXR$^{-/-}$ mice in response to diet

**A–J)** Measurements of hepatic cholesterol (n = 5) (**A**), total plasma cholesterol (n = 3) (**B**), cholesterol in fractionated lipoproteins (n = 3) (**C**), hepatic triglycerides (n = 5) (**D**), plasma triglycerides (n = 3) (**E**), triglycerides in fractionated lipoproteins (n = 5) (**F**), plasma-free fatty acids (n = 3) (**G**), hepatic fatty acid synthesis rates (n = 4) (**H**), plasma leptin (n = 3) (**I**), and plasma insulin (n = 3) (**J**) were taken from wild-type (wt) and LXR$^{-/-}$ mice after feeding different diets (C, chow; W, Western). In (**C**) and (**F**), open triangles refer to chow-fed and closed circles refer to Western-fed mice. Hepatic fatty acid synthesis rates were determined at 17 days, liver chemistries and lipoprotein triglycerides at 7 weeks, and other plasma chemistries at 3 weeks after feeding.

**K)** Glucose tolerance test of wild-type and LXR$^{-/-}$ mice fed a chow diet. After an overnight fast, mice (n = 3 to 5) were injected with 1 g D-glucose/kg body weight, and tail vein glucose was assayed at 15, 30, 45, 60, and 120 min after injection.

VLDL, LDL, IDL, and HDL refer to very low, low, intermediate, and high-density lipoproteins, respectively. *$p < 0.05$, **$p < 0.01$.

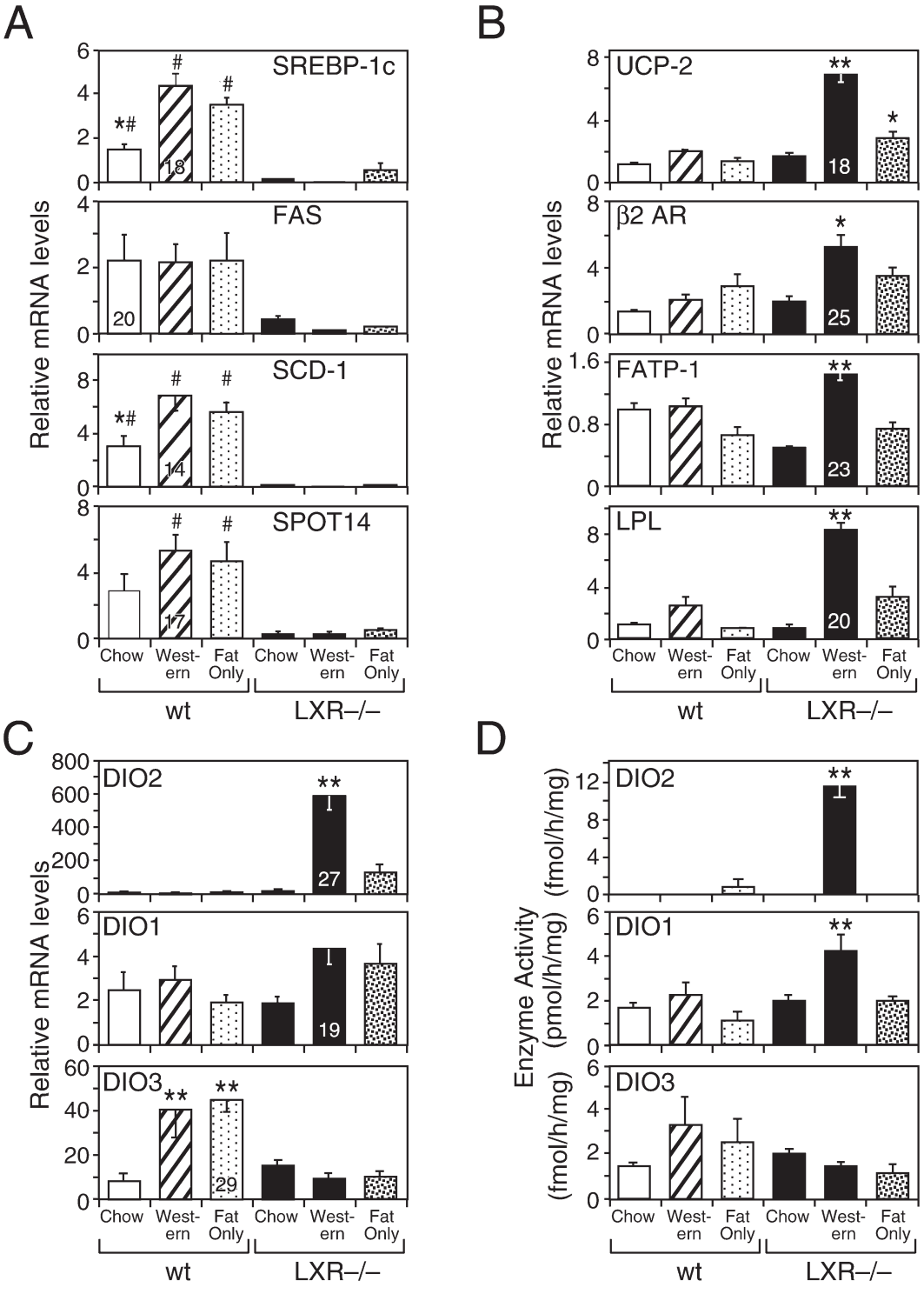


**Figure 3**. Liver gene expression in wild-type and LXR$^{-/-}$ mice in response to diet

**A and B)** mRNA expression of lipogenic genes (**A**) and nonlipogenic thyroid hormone target genes (**B**) in liver of wild-type (wt) and LXR$^{-/-}$ mice (n = 5) fed chow, Western, or high-fat-only diets for 7 weeks.

**C and D)** mRNA expression (**C**) and enzymatic activity (**D**) of type II (DIO2), type I (DIO1), and type III (DIO3) iodothyronine deiodinases in liver of wild-type (wt) and LXR$^{-/-}$ mice fed standard chow, Western, or high-fat-only diets for 7 weeks (n = 5). Cycle time of the highest expressing group for each gene is indicated inside its corresponding bar. mRNA levels were determined by QPCR using the comparative $C_T$ method.

In (**A**), * indicates statistical difference between mice of the same genotype fed different diets, and # indicates statistical difference between this value and that of all mouse groups of the other genotype ($p < 0.05$). In (**B**), (**C**), and (**D**), *$p < 0.05$ and **$p < 0.01$ indicate statistical difference between this and all other values.

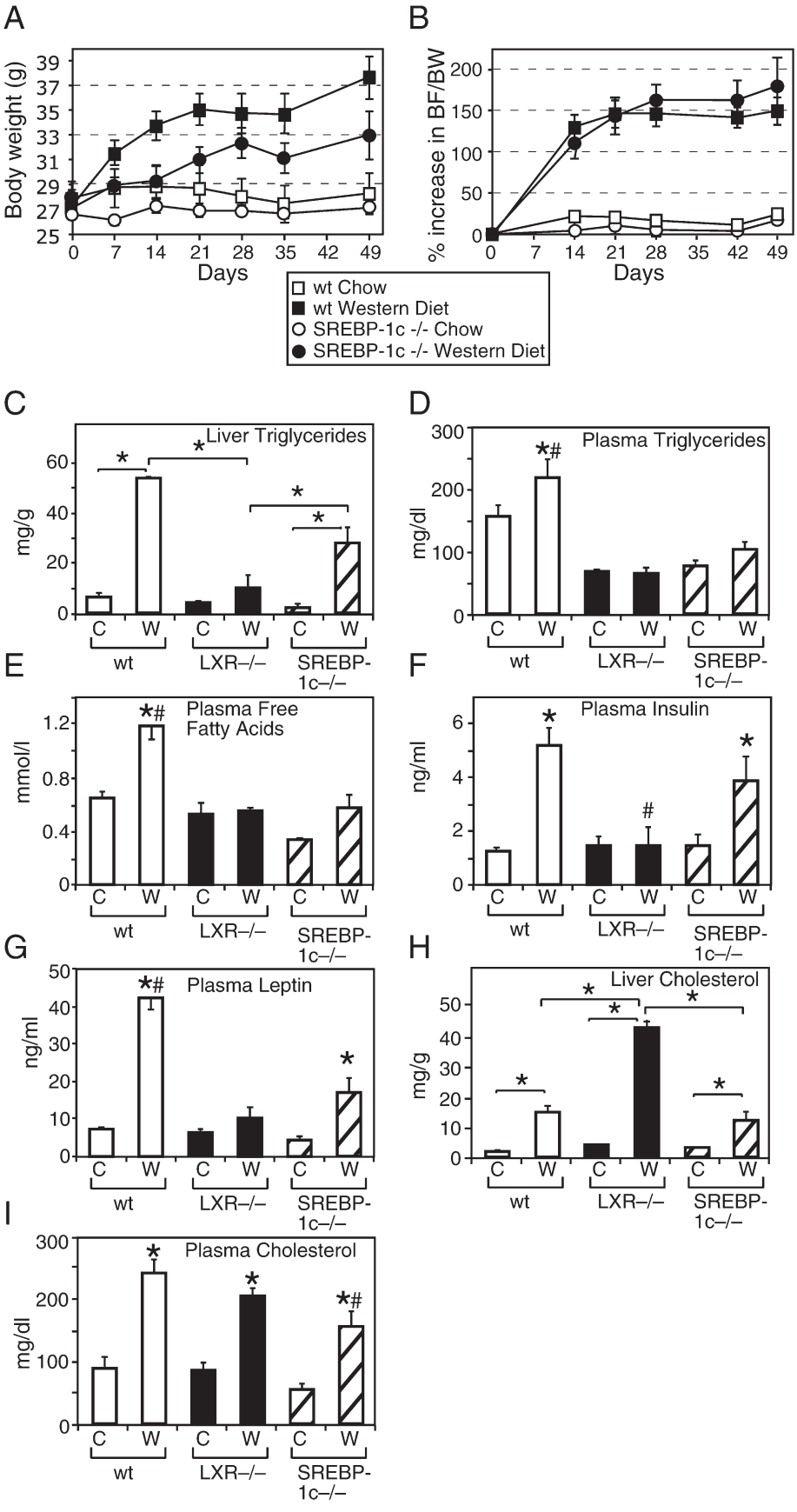


**Figure 4**. Susceptibility to diet-induced obesity in SREBP-1c$^{-/-}$ mice

**A and B)** Growth curves (**A**) and percent increase in body fat over body weight (BF/BW) ratio (**B**) for wild-type (wt) and SREBP-1c$^{-/-}$ mice (n = 6) fed chow versus Western diet for 7 weeks.

**C–I)** Measurements of liver triglycerides (**C**), plasma triglycerides (**D**), plasma-free fatty acids (**E**), plasma insulin (**F**), plasma leptin (**G**), liver cholesterol (**H**), and plasma cholesterol (**I**) were determined from wild-type (wt), LXR$^{-/-}$, and SREBP-1c$^{-/-}$ mice fed for 7 weeks (C, chow; W, Western, n = 5). In (**C**) and (**H**), * indicates $p < 0.01$. In (**D–G**) and (**I**), * indicates statistical significance between animals of the same genotype fed different diets; # indicates significance between this value and that of mice from the other two genotypes ($p < 0.05$).

liver and plasma cholesterol levels were similar in wild-type and SREBP-1c$^{-/-}$ mice on both diets (Figures 4H and 4I). Therefore, the obesity resistance phenotype of LXR$^{-/-}$ mice cannot be explained by the loss of SREBP-1c expression in these animals.

### Cholesterol-dependent thyroid hormone production in LXR$^{-/-}$ mice

In contrast to the fatty acid synthesis genes described above, expression of a limited set of other genes involved in fatty acid utilization (e.g., uncoupling protein-2, *Ucp-2*; β2-adrenergic receptor, *β2AR*; fatty acid transport protein-1, *Fatp-1*; lipoprotein lipase, *Lpl*) were significantly increased in liver of LXR$^{-/-}$ mice but only when both cholesterol and fat were included as part of the diet (Figure 3B). Many of these genes are known targets of thyroid hormone, and, in parallel with their regulation, there was an unprecedented induction of hepatic type II iodothyronine deiodinase (*Dio2*) expression in LXR$^{-/-}$ mice when fed the Western diet but not chow or high-fat-only diets (Figure 3C, top). *Dio2* encodes one of two enzymes that produce active thyroid hormone (T3) from its inactive precursor (T4). DIO2 is the main source of tissue-specific T3 production and is known to deliver the newly synthesized hormone directly to the T3 receptor in the nucleus (reviewed by Bianco et al. [2002]). Although not normally expressed in liver, hepatic DIO2 mRNA levels found in LXR$^{-/-}$ mice on the Western diet were comparable to those in wild-type skeletal muscle (Figure 5A) but less than in wild-type brown fat on the same diet (Figure S1B). In accordance with mRNA levels, hepatic DIO2 enzyme activity was also markedly induced in LXR$^{-/-}$ mice fed only the Western diet (Figure 3D, top). Type I deiodinase (DIO1), which is known to be autoregulated by T3, was also increased slightly (Figures 3C and 3D, middle). No differences were detected in the deactivating, type III deiodinase (DIO3) (Figures 3C and 3D, bottom). Interestingly, despite the level of DIO2 in liver, no changes in plasma T3, T4, or thyroid-stimulating hormone levels were detected (data not shown), consistent with the well-documented role of DIO2 in elevating tissue T3 levels and affecting T3 target genes without influencing plasma T3 levels (de Jesus et al., 2001; Pachucki et al., 2001; Schneider et al., 2001). Importantly, T3 target genes involved in lipogenesis (*Fas*, *Acc*, *Scd-1*, *Me*, ATP-citrate lyase [*Acl*], glycerol-3-phosphate acyltransferase [*Gpat*], *Spot14*) were not induced but downregulated in LXR$^{-/-}$ mice (Figure 3A; Figure S1A). This observation was consistent with the low level of SREBP-1c in these mice, which is required for thyroid hormone regulation of lipogenic target genes such as *Spot14* (Jump et al., 2001).

### Increased energy expenditure and uncoupled oxidative phosphorylation in LXR$^{-/-}$ mice

Real-time QPCR analysis in peripheral tissues revealed a striking, atypical increase in expression of genes involved in fat utilization in skeletal muscle and white fat (Figure 5). In particular, we observed the strong, abnormal expression of uncoupling protein-1 (UCP-1) in LXR$^{-/-}$ mice under all dietary conditions, although the levels were 2- to 3-fold higher in animals on the high-fat diets (Figure 6A; Figure S2A). UCP-1 is the mitochondrial protein that uncouples respiration and oxidative phosphorylation in brown fat, but it is not normally expressed in muscle or white fat. Comparing tissues, muscle UCP-1 mRNA achieved levels 25- to 55-fold higher than white adipose (Figure 6A). UCP-1 protein expression in LXR$^{-/-}$ skeletal muscle was confirmed by immunoblot analysis of mitochondrial protein fractions at 4% the level found in brown fat (Figure 6B). In contrast, no UCP-1 protein was detected in wild-type animals on any of the diets (Figure 6B). Although ectopic expression of some brown adipose cells in the LXR$^{-/-}$ muscle mass could not be completely ruled out, we note that no other adipose-specific genes (e.g., adipocyte fatty acid binding protein, *aP2*) were comparably elevated in these samples (Figure 6A). In addition, histological examination of skeletal muscle from mice on the Western diet revealed substantially fewer fat cells between muscle fibers in LXR$^{-/-}$ versus wild-type mice (Figure 6C). Supporting this analysis, direct measurement of mitochondrial respiration from dissected muscle fibers revealed that respiration control ratios were significantly lower in LXR$^{-/-}$ mice, demonstrating that uncoupled respiration was increased in muscle (Figure 6D).

An intriguing aspect of UCP-1 induction in skeletal muscle and white fat was that it occurred independent of increasing the PPARγ coactivators PGC1α and β (Figure 5), which are believed to be required for UCP-1 expression in brown fat. In conjunction with increased uncoupling, genes involved in fatty acid and triglyceride synthesis (*Fas*, *Acc*, *Scd-1*, glycerol kinase [*Gyk*]) and import (fatty acid transport protein-2, *Fatp-2*) were upregulated in muscle from LXR$^{-/-}$ mice on the Western (Figure 5A) and high-fat-only diets (data not shown). This regulation occurred despite decreased expression of SREBP-1c, consistent with the suggestion that lipid metabolism is governed differently by LXRs in muscle compared to liver (Muscat et al., 2002). In contrast, SREBP-1c expression in adipose tissue increased in LXR$^{-/-}$ mice, demonstrating that LXRs are not required for basal SREBP-1c expression in adipose tissues (Figure 5B). Surprisingly, no changes in oxidative gene expression (including *Ucp-1*), histology, or morphology were observed in brown fat, suggesting that this tissue does not contribute to the resistance phenotype (Figure S1B and data not shown).

The results above suggested that the resistance to weight gain observed in LXR$^{-/-}$ mice might have been due to increased energy expenditure. To examine this possibility, wild-type and LXR$^{-/-}$ mice were housed in metabolic cages and assayed for oxygen consumption after feeding normal chow versus high-fat diets. In comparison to wild-type littermates, LXR$^{-/-}$ mice exhibited a 19% (nighttime) to 27% (daytime) increase in oxygen consumption. This increase became more significant (>30% over wild-type) during both the day (resting period) and night (active period) when the animals were fed both the Western and the high-fat-only diets (Figure 6E and Figure S2B), demonstrating that LXR$^{-/-}$ mice are in a greatly elevated oxidative state. The finding that fasting plasma ketone bodies were not changed in LXR$^{-/-}$ mice (data not shown) was further evidence that this energy consumption was occurring within peripheral tissues.

### Increased fatty acid synthesis in peripheral tissues compensates for increased energy consumption in LXR$^{-/-}$ mice fed high-fat-only but not Western diet

The finding that LXR$^{-/-}$ mice expend substantially more energy in their peripheral tissues provides a convincing explanation for why these animals are resistant to obesity on a Western diet that includes both fat and cholesterol. However, these findings do not explain why LXR$^{-/-}$ mice fed a high-fat-only diet (with-

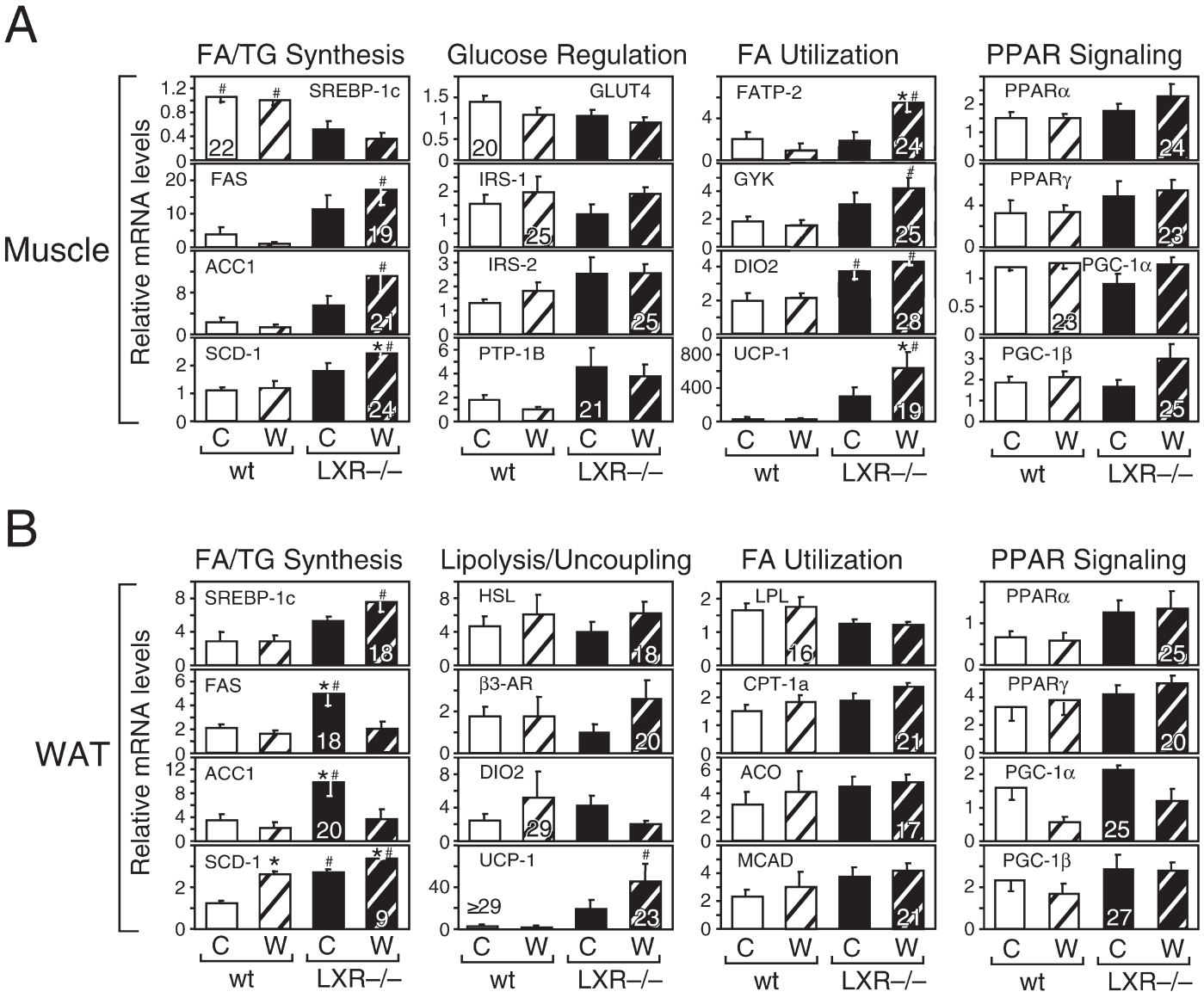


**Figure 5**. Comparative expression analysis of genes involved in lipid and glucose metabolism in muscle and white adipose of wild-type and LXR$^{-/-}$ mice in response to diet

**A and B)** QPCR using the comparative $C_T$ method was performed on RNA extracted from skeletal muscle (rectus femoris) (**A**), and white adipose tissue (WAT) (**B**) of wild-type (wt) and LXR$^{-/-}$ mice fed for 7 weeks (C, chow; W, Western). The cycle time of the highest expressing group for each gene analyzed is indicated inside its corresponding bar. * indicates statistical significance between animals of the same genotype fed different diets; # indicates significance between wild-type and LXR$^{-/-}$ mice fed the same diet ($p < 0.05$, $n = 5$). *Glut4*, glucose transporter 4; *Hsl*, hormone sensitive lipase; *Irs-1/2*, insulin receptor substrate 1/2; *Mcad*, medium-chain acyl-CoA dehydrogenase; *Ptp-1b*, protein-tyrosine phosphatase-1B. Abbreviations for other genes are defined in the text.

out cholesterol) are still susceptible to obesity, since these mice exhibited similar increases in UCP-1 and energy consumption regardless of diet (compare Figure 6 to Figure S2). Therefore, a compensatory mechanism must exist in LXR$^{-/-}$ mice on the high-fat-only diet to permit them to gain weight in spite of abnormally high energy loss. In Figures 7A and 7B, we show that this compensation may be explained by a large, unexpected increase in fatty acid synthesis in muscle (3-fold) and white adipose tissue (4-fold) that occurred on the high-fat-only diet but not on chow or Western diets. The absolute rates of synthesis, particularly in white adipose, were enough to account for the weight gain on the high-fat-only diet. Interestingly, fatty acid synthesis in liver remained substantially lower in LXR$^{-/-}$ mice, regardless of diet (Figure 7C).

## Discussion

### LXRs as a model for obesity resistance

In this paper, the role of LXRs in regulating dietary fat metabolism was investigated. Using complementary metabolic and biochemical approaches, we show that LXR$^{-/-}$ mice are resistant to diet-induced obesity by a mechanism that differs from

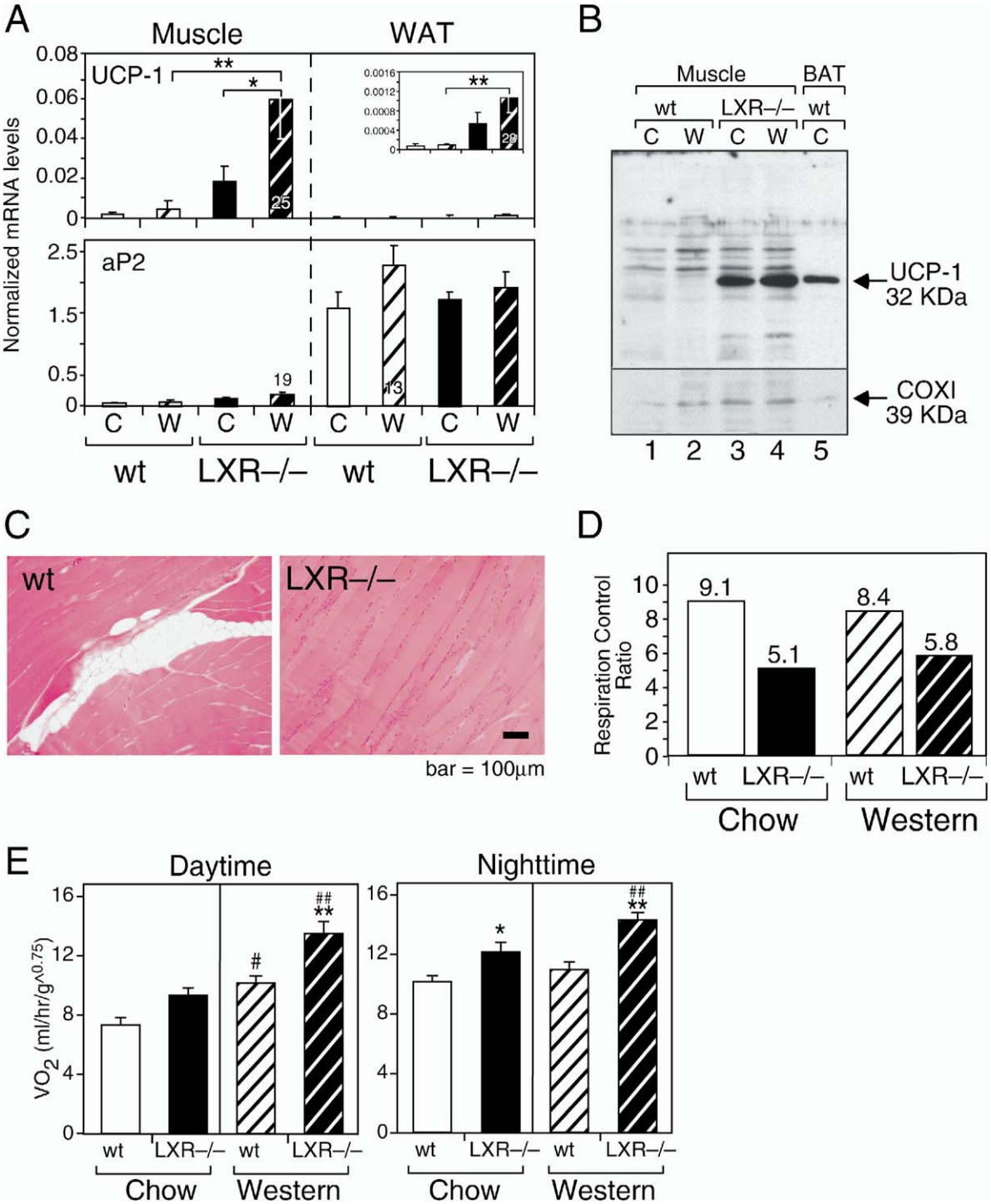


**Figure 6**. Increased metabolic rate and uncoupling of oxidative phosphorylation in LXR$^{-/-}$ mice

**A)** QPCR analysis (standard curve method) comparing expression of *Ucp-1* and *aP2* in rectus femoris muscle versus white adipose tissue (WAT) from wild-type (wt) and LXR$^{-/-}$ mice after 7 weeks of feeding (C, chow; W, Western). The cycle time of the highest expressing group for each gene analyzed is indicated inside its corresponding bar. *$p < 0.05$, **$p < 0.01$, n = 5.

**B)** Immunoblot analysis of mitochondrial UCP-1 from wild-type and LXR$^{-/-}$ mice treated as in (A). Lanes 1–4, protein extracts (100 μg) from rectus femoris muscle; lane 5, protein extract (2 μg) from brown adipose tissue (BAT). Protein loading was confirmed by stripping and reprobing the blot with cytochrome C oxidase antibody as a control.

**C)** Histology of rectus femoris muscle from wild-type and LXR$^{-/-}$ mice fed a Western diet for 7 weeks. The slides stained by hematoxyline and eosin show accumulation of fat cells in between muscle fibers in wild-type but not LXR$^{-/-}$ mice and are representative of all fields in samples from several animals. Scale bar, 100 μm.

**D)** Respiration control ratios measured from rectus femoris muscle mitochondrial extracts of wild-type and LXR$^{-/-}$ mice fed standard chow or Western diets for 3 weeks. Extracts were pooled from three animals, and the data are representative of duplicate experiments.

**E)** Oxygen consumption ($VO_2$) was measured in wild-type (wt) and LXR$^{-/-}$ mice during daytime (resting) and nighttime (active) during week 4 of feeding a chow or Western diet (n = 4). *$p < 0.05$ and **$p < 0.01$ indicate statistical significance between wild-type and LXR$^{-/-}$ mice fed the same diet. $^{\#}p < 0.05$ and $^{\#\#}p < 0.01$ indicate statistical significance between animals of the same genotype fed different diets.

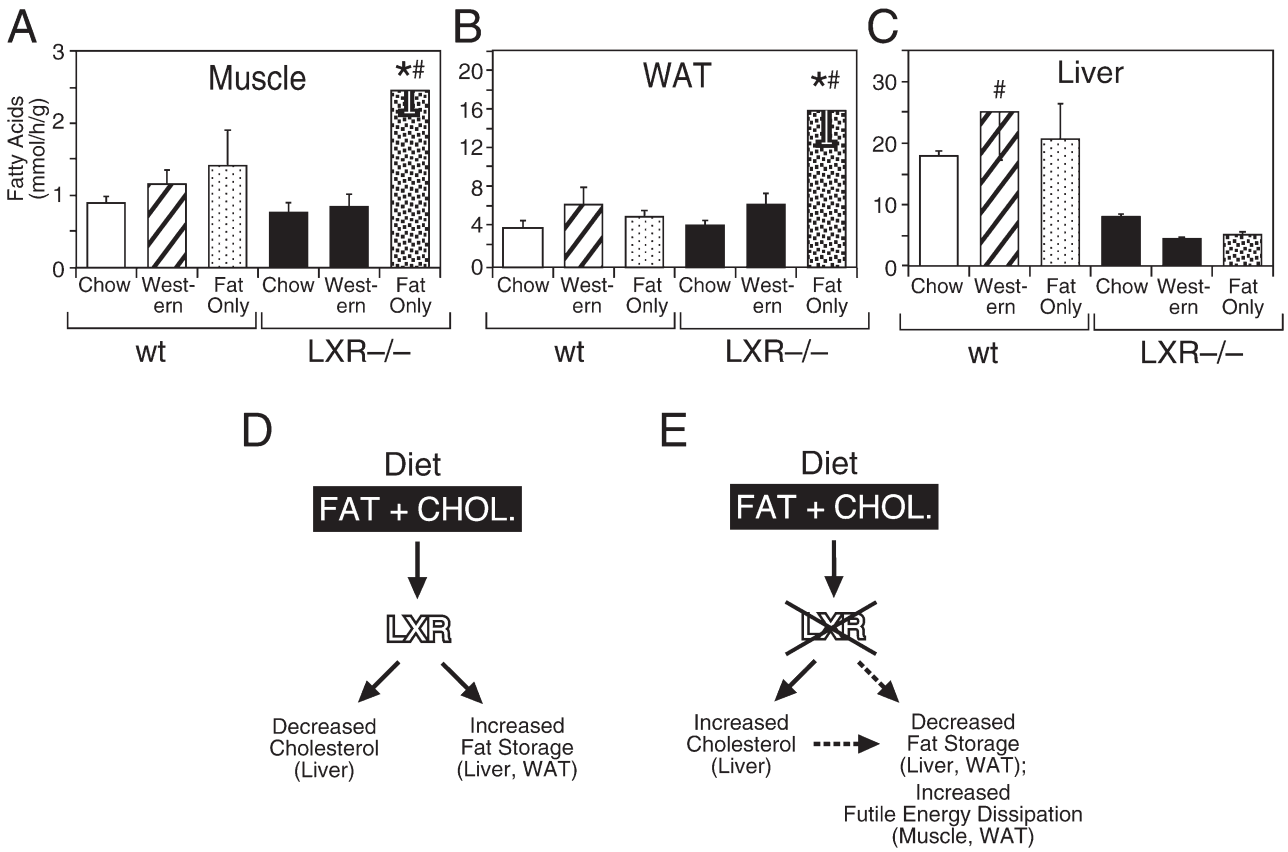


**Figure 7**. Lipogenesis in peripheral tissues of wild-type and LXR$^{-/-}$ mice and a model for the dual regulatory role of LXRs in dietary cholesterol and fat metabolism

**A–C)** Fatty acid synthesis rates in skeletal muscle (**A**), white adipose (WAT) (**B**), and liver (**C**) were determined in wild-type and LXR$^{-/-}$ mice fed either chow, Western, or high-fat-only diet for 17 days (n = 4). * indicates statistical difference between this value and that of mice of the same genotype fed different diets; # indicates statistical significance between this value and that of all mouse groups of the other genotype ($p < 0.05$).

**D)** By sensing the cholesterol component of a lipid-rich diet, LXRs prevent accumulation of excess cholesterol and permit storage of dietary fat.

**E)** In the absence of LXRs, the balance between fat storage and oxidation is altered, and the accumulation of hepatic cholesterol now drives peripheral tissues to aberrantly dissipate fat-derived energy.

other animal models of obesity resistance (Chen and Farese, 2001; Yuan et al., 2001; Ntambi et al., 2002; Kamei et al., 2003; Wang et al., 2003; Um et al., 2004). One factor that contributes to this phenotype is the defect LXR$^{-/-}$ mice have in hepatic lipogenesis. Even on a standard chow diet, LXR$^{-/-}$ mice weighed less (Figure 1), had lower hepatic and plasma lipid levels, and were unable to properly synthesize fatty acids and triglycerides or store them in liver and adipose tissue (Figure 2). These defects are due in large part to LXR's role as a regulator of the hepatic SREBP-1c transcriptional cascade that is normally activated upon feeding but is almost entirely absent in LXR$^{-/-}$ animals (Figure 3A). However, just the loss of SREBP-mediated lipogenesis in LXR$^{-/-}$ mice is not enough to explain fully the inability of these animals to gain weight on a Western high-fat, high-cholesterol diet. This conclusion is based on our observation that SREBP-1c null mice do not recapitulate the obesity resistance phenotype, regardless of diet (Figure 4), and suggests that a separate defect underlies the fate of the dietary fat in LXR$^{-/-}$ mice.

In addition to their lean body mass, the LXR$^{-/-}$ mice displayed an abnormally high metabolic rate compared to their wild-type littermates (Figure 6E). This lean and hypermetabolic basal phenotype of LXR$^{-/-}$ mice is reminiscent of the phenotype described in mice lacking SCD-1 (Cohen et al., 2002; Ntambi et al., 2002; Dobrzyn et al., 2004). *Scd-1* is a downstream target of the LXR/SREBP-1c transcriptional cascade (Repa et al., 2000a). Indeed, hepatic SCD-1 mRNA levels were decreased substantially in LXR$^{-/-}$ mice regardless of diet (Figure 3A), suggesting that at least part of the basal LXR$^{-/-}$ phenotype might be due to decreased SCD-1. Although there are also clear differences between the LXR and SCD-1 knockout models (e.g., liver fatty acid oxidation was elevated in SCD-1$^{-/-}$ but not LXR$^{-/-}$ mice), it will be of interest to test whether mice lacking SCD-1 exhibit a similar increase in uncoupled oxidative phosphorylation in muscle and adipose as that found in LXR$^{-/-}$ mice.

### Where does the fat go?

Another unusual feature of the LXR null mice was that they maintained substantially lower circulating plasma triglycerides and displayed almost undetectable levels of plasma VLDL triglycerides even when fed the high-fat/high-cholesterol West-

ern diet. Since both *Lpl* and *Fatp-1* were upregulated in liver of LXR$^{-/-}$ mice in a cholesterol-dependent manner, another process that may contribute to lower plasma triglycerides is their incorporation into cholesterol esters in liver. Because the normal endogenous lipogenic pathway is impaired in LXR$^{-/-}$ mice, an increase in hepatic triglyceride uptake would be required to esterify the large amounts of cholesterol that accumulated due to defective elimination of hepatic cholesterol. However, esterification would not be expected to completely prevent peripheral fat storage and obesity in LXR$^{-/-}$ mice, since this process can only account for a fraction of the total dietary fat and in any case would favor an increase rather than a steady state or decrease in total body weight.

A more plausible explanation for the low levels of circulating triglycerides and obesity resistance in LXR$^{-/-}$ mice is that the dietary fat is taken up and burned in peripheral tissues. This conclusion is strongly supported by the unprecedented upregulation of UCP-1 expression and uncoupled oxidative phosphorylation in muscle and adipose, and the marked increase in metabolic rate observed in LXR$^{-/-}$ mice (Figure 6). Although the reason for the unexpected UCP-1 expression in LXR$^{-/-}$ mice requires further investigation, its relevance to the observed phenotype has been confirmed by earlier studies showing that similar levels of ectopic UCP-1 expression in either muscle or adipose tissue of transgenic mice also caused increased energy expenditure and prevented obesity (Kopecky et al., 1995; Kopecky et al., 1996; Li et al., 2000). Another unprecedented finding in the LXR$^{-/-}$ animals was that their increased energy expenditure was not associated with changes in brown adipose (Figure S1B) or the expression of PGC1$\alpha$ or PGC1$\beta$ (Figure 5), the coregulatory transcription factors that normally function as metabolic switches that lead to fat oxidation (Lin et al., 2003; Puigserver and Spiegelman, 2003).

**What is the cholesterol-derived signal?**

Perhaps the most distinguishing and striking feature of the LXR$^{-/-}$ phenotype is the requirement for dietary cholesterol to promote obesity resistance upon high fat intake (Figure 1). Indeed, when the LXR null mice were fed a high-fat diet that did not contain cholesterol, these animals gained weight similar to their wild-type littermates. Since defective hepatic lipogenesis and increased energy expenditure were observed in all LXR$^{-/-}$ animals (regardless of diet), some compensatory pathway must have existed to overcome the high level of fat oxidation in these animals when they were fed a high-fat diet without cholesterol. Our results indicate that at least two diet-specific phenotypes likely accounted for the cholesterol-dependent resistance to obesity in LXR$^{-/-}$ mice. First, we found a substantial compensatory increase in fatty acid synthesis in muscle and white adipose of LXR$^{-/-}$ mice fed a high-fat-only but not Western diet (Figures 7A and 7B). The high level of fat production in these tissues was enough to explain the weight gain in these animals. This unusual compensatory mechanism for the maintenance of body lipids is reminiscent of a similar finding reported for the liver-specific SREBP cleavage-activating protein (SCAP) knockout mice (Kuriyama et al., 2005). These mice were suggested to compensate for their decreased hepatic fatty acid synthesis by exhibiting a balanced increase in synthesis in peripheral tissues, primarily adipose.

The second diet-specific phenotype we observed was the increased production of active thyroid hormone from its inactive precursor in liver due to ectopic expression and activity of DIO2. This abnormal expression of DIO2 occurred only in LXR$^{-/-}$ mice fed the Western diet and was not present when animals were fed only high fat (Figure 3) or only high cholesterol (data not shown). Given the well-characterized role of DIO2 induction in controlling adaptive energy expenditure (Bianco and Silva, 1987), ectopic expression of DIO2 in LXR$^{-/-}$ mice would be expected to have noticeable effects in liver. Consistent with this idea, target genes involved in fatty acid transport and metabolism were increased significantly (*Fatp-1*, *B2AR*, *Ucp-2*, *Lpl*) in liver from LXR$^{-/-}$ mice on a Western diet (Figure 3B). At present, it remains unclear how cholesterol regulates *Dio2* expression in LXR$^{-/-}$ mice or how this regulation might suppress the compensatory fatty acid synthesis rates seen in the periphery of LXR$^{-/-}$ animals that lack the cholesterol component of a high-fat diet. The mechanism of this aberrant regulation and the possible involvement of other sterol-regulated transcription factors such as SREBP-1a and SREBP-2 are under investigation. Although the metabolic changes taking place in the periphery and those observed in the liver of LXR$^{-/-}$ mice on Western diet might constitute two independent, unrelated events, it is possible that these processes, like many others in animal physiology, are interconnected and integrate together to affect systemic homeostasis. Because liver is the major site for processing dietary lipids and undergoes dramatic cholesterol-induced metabolic changes in LXR$^{-/-}$ animals (e.g., cholesterol accumulation, altered bile acid metabolism, and gene expression changes), it is reasonable to conclude that the liver may be the source of the cholesterol-derived signal.

**LXRs integrate cholesterol and triglyceride homeostasis**

The data presented here support a model in which LXRs' regulation of fat metabolism is integrated through their key role in maintaining cholesterol homeostasis (Figure 7D). Previous work has shown that LXRs act as sterol sensors and limit cholesterol accumulation by decreasing its absorption and increasing its reverse transport and catabolism (reviewed in Repa and Mangelsdorf [2002]). At the same time, activation of the LXR pathway by dietary cholesterol would be expected to stimulate hepatic triglyceride synthesis and fat storage by upregulating the SREBP-1c metabolic cascade and mimicking the effects of insulin. In agreement with this latter conclusion, we and others have shown that LXRs are required for both the basal expression (Figure 3A; Repa et al. [2000a]) and the insulin-induced expression (Chen et al., 2004) of SREBP-1c and its downstream target genes. LXRs have also been implicated in hepatic carbohydrate metabolism by stimulating genes involved in glucose storage and inhibiting gluconeogenesis (Figure S1A, Cao et al. [2003], Dalen et al. [2003], Laffitte et al. [2003]), which would be consistent with their role in promoting energy storage. In the LXR$^{-/-}$ animals, these pathways are missing, and the increased accumulation of sterols along with the aberrant increase in oxidative gene expression now shift the energy balance toward dissipation rather than storage (Figure 7E). Thus, from an evolutionary point of view, the LXRs have solved the important metabolic conundrum of how to limit the accumulation of cholesterol, which animals can synthesize themselves,

and at the same time permit the deposition of fat as an energy-rich fuel source.

## Experimental procedures

### Animal experiments

Wild-type, LXRα/β knockout mice ($LXR^{-/-}$) (Peet et al., 1998; Repa et al., 2000b) and SREBP-1c knockout mice ($SREBP\text{-}1c^{-/-}$ provided by Drs. Brown and Goldstein) (Liang et al., 2002) were maintained in a mixed strain background (C57BL/6:129 SvEv) and housed in a temperature-controlled environment with 12 hr light/dark cycles. Age-matched (4–5 months old) male mice had free access to water and were fed ad libitum (for 3 or 7 weeks) from one of three diets: standard rodent chow (TD 7001, Harlan Teklad, Madison, WI) that contains 4% (w/w) total lipid (<12% of its calories as animal fat) and ≤0.04% (w/w) cholesterol; a Western-style diet (TD 88137, Harlan Teklad, Madison, WI) containing 21% (w/w) total lipid (42% calories as anhydrous milk fat [65% saturated, 32% monounsaturated, 3% polyunsaturated fats]) and 0.2% (w/w) total cholesterol (of which 0.05% is contributed by milk fat and 0.15% is added); or a high-fat-only diet, which has the same constituents as the Western diet but lacks additional cholesterol. Body weight was recorded weekly, and food intake was measured biweekly. Total body fat mass was analyzed weekly by NMR using the Minispec mq spectrometer (Bruker). At the end of the feeding period, mice were anesthetized with halothane and exsanguinated via the ascending vena cava prior to organ harvest. Blood was kept on ice in heparin-coated tubes (Microvette 500 LH; Sarstedt, Inc.) and centrifuged (1500 × g for 15 min at 4°C), and the plasma was stored at –20°C until analysis. For lipoprotein and TSH measurements, blood was collected in EDTA-coated tubes. Plasma for lipoprotein measurements was kept at 4°C in the presence of protease inhibitors prior to analysis. Tissues were harvested for analyses as described below. All experiments were approved by the Institutional Animal Care and Research Advisory Committee at the University of Texas Southwestern Medical Center.

### Lipid absorption

On week 5 of the dietary study, stools were collected from individually housed mice over 72 hr. Lipid content of diets and stools was determined gravimetrically and used to calculate the fraction of consumed lipid that was absorbed as described in Figure 1D (Schwarz et al., 1998).

### Liver triglycerides and cholesterol

Cholesterol was extracted from saponified liver (0.3 g) with petroleum ether and quantitated by gas chromatography using stigmasterol as an internal standard. Other lipids were extracted from liver (0.2 g) in chloroform:methanol (2:1, v/v). Extracts were then washed once in 50 mM NaCl and twice in 0.36 M $CaCl_2$/methanol. The organic phase was separated and brought up to 5 ml with chloroform. Ten microliters of chloroform:Triton X-114 (1:1, v/v) was added to duplicate 100 μl aliquots of each extract and standards (Sigma Diagnostics), which were then air dried overnight. Colorimetric enzymatic assays were performed using 1 ml triglyceride reagent (ThermoTrace). After 20 min, optical densities of each sample were read at 520 nm and compared to prepared standards.

### In vivo measurements of hepatic fatty acid synthesis

Rates of fatty acid synthesis were measured in liver, skeletal muscle (hindlimb), and epididymal white adipose tissue of wild-type and $LXR^{-/-}$ mice during the early light cycle as described (Horton et al., 1998).

### Plasma analyses and glucose tolerance

For glucose tolerance, mice were fasted overnight before receiving an intraperitoneal injection of 20% D-glucose (Sigma) (1 g/kg body weight). At 0, 15, 30, 45, 60, and 120 min after injection, 5–10 μl of blood was drawn from the tail and blood glucose levels assayed using an Elite XL Glucometer (Bayer). For other plasma chemistry analyses, two measurements were performed: one with and one without a 4 hr fast. Different enzymatic assays were used for each analyte, including total cholesterol (Roche Diagnostics), plasma triglycerides (ThermoTrace), free fatty acids (Roche), insulin (CrystalChem), leptin (CrystalChem), ketone bodies (Ranbut, Randox), and total T3/T4 (DPC Coat-A-Count). Plasma lipoprotein levels were analyzed by fast protein liquid chromatography using two serial Superose HR6 columns, followed by enzymatic analysis of their cholesterol and triglyceride contents using the kits described above. TSH levels were determined by RIA using an anti-mouse TSH antibody at the National Hormone and Pituitary Program (Dr. A.F. Parlow, Harbor-UCLA Medical Center).

### Calorimetry measurements

Utilizing a modified Oxymax system (Columbus Instruments, Columbus, OH), a series of ten airtight calorimetric chambers were engineered to assess the metabolic activity of mice over one 12 hr light/12 hr dark cycle. Two empty chambers served as reference controls. Standard gas mixtures of $O_2$, $CO_2$, and $N_2$ were used to calibrate the system prior to the initiation of each experiment. Room air gas was infused into each chamber at a rate of 415 cc/min. Every 30 min, $O_2$ and $CO_2$ concentrations were measured in each chamber, and oxygen consumption ($VO_2$) and carbon dioxide production ($VCO_2$) were calculated and averaged for the light and dark cycle for each mouse. Mice were analyzed in two sets over consecutive days (eight mice per set, four per genotype from two diets) in individual calorimeter chambers containing water, food (chow versus high-fat diets) maintained at constant temperature and humidity. Baseline data were collected prior to the initiation of the special food diet and then every 2 weeks (for a total of 6 weeks) after randomization to one of the two food diets.

### Real-time PCR analysis

Total RNA was extracted from tissues using RNA STAT-60 (Tel-Test, Inc.), treated with DNase I (RNase-free, Roche Molecular Biochemicals), and reverse transcribed into cDNA with random hexamers using the SuperScript II First-Strand Synthesis System (Invitrogen). Primers for each mRNA were designed using Primer Express Software (PerkinElmer Life Sciences) based on sequence data from GenBankTM (Table S1) and were validated as described (Bookout and Mangelsdorf, 2003). Real-time PCR reactions contained 10–25 ng cDNA, 150 nM of each primer, and 5 μl 2X-Jump Start SYBR Green PCR Master Mix (Sigma) in 10 μl total volume. PCR reactions were performed in triplicate using an Applied Biosystems Prism 7900HT instrument. Relative mRNA levels were calculated using either the comparative $C_T$ or standard curve methods normalized to cyclophilin mRNA or 18S RNA, respectively.

### Deiodinase activity assay

Deiodinase activities were assayed as described (Curcio-Morelli et al., 2003) in the presence of 20 mM DTT for DIO1 and DIO2 and 10 mM DTT for D3. Briefly, tissue fragments were sonicated in 0.1 M $K_2PO_4$, 1 mM EDTA (pH 6.9) containing DTT and 0.25 M sucrose. Each sample (200 μg protein) was assayed in duplicate using 0.5 nM or 100 nM $^{125}$I-T4 (NEN Life Science Products, Inc., Boston, MA). Catalytic activities of both DIO1 and DIO2 are detected in the presence of 0.5 nM $^{125}$I-T4, but only DIO1 activity is detected in the presence of 100 nM $^{125}$I-T4. DIO2 activity was calculated based on the difference of $^{125}$I produced between the two conditions. A similar approach was used to measure DIO3 activity, except that 0.1 nM $^{125}$I-T3 (NEN Life Science Products, Inc., Boston, MA) was used as substrate. All results were corrected for random deiodination.

### Western blotting

Mitochondrial protein fractions were prepared as described (Bhattacharya et al., 1991) from skeletal muscle and interscapular brown adipose tissue, resolved on a 12% SDS-polyacrylamide gel, and electrotransferred to a PVDF membrane (Amersham). The membrane was then hybridized with rabbit anti-mouse UCP-1 antiserum (recognizing the C terminus of mouse and rat UCP-1) (Alpha Diagnostic International, San Antonio) at a 1:3000 dilution, followed by secondary antibody incubation at a 1:5000 dilution. UCP-1-specific bands were detected by chemiluminescence (ECL kit, Amersham).

### Histological procedures

Rectus femoris muscle was fixed in formalin (Accustain, Sigma), embedded in paraffin wax, sectioned, and stained with hematoxylin and eosin. Sections were examined under bright-field microscopy at 100× magnification.

### Muscle mitochondrial respiration

Purified mitochondrial fractions were prepared as described (Bhattacharya et al., 1991) and resuspended in the presence of 0.5% BSA. Fractions con-

taining 1 mg protein were injected into a magnetically stirred sample chamber of a model 110 fiberoptic oxygen monitor (Instech Laboratories, Plymouth Meeting, PA). Oxygen consumption was then recorded continuously for 15 min, during which the following were sequentially injected into the chamber: 3 mM each of malate and glutamate (Sigma), followed by 270 μM ADP and 540 μM ADP (Sigma). As a control, 2 μM of the reducing agent carbonyl cyanide chlorophenylhydrazone (Sigma) was injected followed by 540 μM ADP. Respiration control ratios were quantitated according to Estabrook (1967).

### Statistical analyses

Values are expressed as mean ± standard error of the mean. Significant differences between mean values were evaluated using two-tailed, unpaired Student's t test (when two groups were analyzed) or one-way ANOVA followed by Student Newman-Keuls test (for three or more groups).

### Supplemental Data

Supplemental Data include two figures and one table and can be found with this article online at http://www.cellmetabolism.org/cgi/content/full/1/4/231/DC1/.

### Acknowledgments

We thank Drs. Michael Brown and Joseph Goldstein for SREBP-1c$^{-/-}$ mice; Antonio Moschetta, Steve Kliewer, Joyce Repa, Oleg Guryev, Ronald Estabrook, Cai Li, Stephen Turley, and Helen Hobbs for comments and suggestions; Norma Anderson, Amy Liverman, Angie Bookout, and Stacie Cary for help on experiments; and members of the Mango lab for helpful suggestions. D.J.M is an investigator, and K.C.G. is an associate of the Howard Hughes Medical Institute. This work was funded by the Howard Hughes Medical Institute, the Robert A. Welch Foundation, and National Institutes of Health grants (U19DK62434 and P20RR20691). D.J.M. serves as a consultant for Exelixis, Inc.

Received: September 28, 2004
Revised: February 9, 2005
Accepted: March 2, 2005
Published: April 12, 2005

### References

Abu-Elheiga, L., Oh, W., Kordari, P., and Wakil, S.J. (2003). Acetyl-CoA carboxylase 2 mutant mice are protected against obesity and diabetes induced by high-fat/high-carbohydrate diets. Proc. Natl. Acad. Sci. USA *100*, 10207–10212.

Bhattacharya, S.K., Thakar, J.H., Johnson, P.L., and Shanklin, D.R. (1991). Isolation of skeletal muscle mitochondria from hamsters using an ionic medium containing ethylenediaminetetraacetic acid and nagarse. Anal. Biochem. *192*, 344–349.

Bianco, A.C., and Silva, J.E. (1987). Intracellular conversion of thyroxine to triiodothyronine is required for the optimal thermogenic function of brown adipose tissue. J. Clin. Invest. *79*, 295–300.

Bianco, A.C., Salvatore, D., Gereben, B., Berry, M.J., and Larsen, P.R. (2002). Biochemistry, cellular and molecular biology, and physiological roles of the iodothyronine selenodeiodinases. Endocr. Rev. *23*, 38–89.

Bookout, A.L., and Mangelsdorf, D.J. (2003). A quantitative real-time PCR protocol for analysis of nuclear receptor signaling pathways. NURSA e-Journal *1*, ID 1.11082003.1.

Cao, G., Liang, Y., Broderick, C.L., Oldham, B.A., Beyer, T.P., Schmidt, R.J., Zhang, Y., Stayrook, K.R., Suen, C., Otto, K.A., et al. (2003). Antidiabetic action of a liver x receptor agonist mediated by inhibition of hepatic gluconeogenesis. J. Biol. Chem. *278*, 1131–1136.

Chawla, A., Repa, J.J., Evans, R.M., and Mangelsdorf, D.J. (2001). Nuclear receptors and lipid physiology: opening the X-files. Science *294*, 1866–1870.

Chen, H.C., and Farese, R.V., Jr. (2001). Turning WAT into BAT gets rid of fat. Nat. Med. *7*, 1102–1103.

Chen, G., Liang, G., Ou, J., Goldstein, J.L., and Brown, M.S. (2004). Central role for liver X receptor in insulin-mediated activation of Srebp-1c transcription and stimulation of fatty acid synthesis in liver. Proc. Natl. Acad. Sci. USA *101*, 11245–11250.

Clapham, J.C., Arch, J.R., Chapman, H., Haynes, A., Lister, C., Moore, G.B., Piercy, V., Carter, S.A., Lehner, I., Smith, S.A., et al. (2000). Mice overexpressing human uncoupling protein-3 in skeletal muscle are hyperphagic and lean. Nature *406*, 415–418.

Cohen, P., Miyazaki, M., Socci, N.D., Hagge-Greenberg, A., Liedtke, W., Soukas, A.A., Sharma, R., Hudgins, L.C., Ntambi, J.M., and Friedman, J.M. (2002). Role of stearoyl-CoA desaturase-1 in leptin-mediated weight loss. Science *297*, 240–243.

Curcio-Morelli, C., Gereben, B., Zavacki, A.M., Kim, B.W., Huang, S., Harney, J.W., Larsen, P.R., and Bianco, A.C. (2003). In vivo dimerization of types *1*, 2, and 3 iodothyronine selenodeiodinases. Endocrinology *144*, 937–946.

Dalen, K.T., Ulven, S.M., Bamberg, K., Gustafsson, J.A., and Nebb, H.I. (2003). Expression of the insulin-responsive glucose transporter GLUT4 in adipocytes is dependent on liver X receptor alpha. J. Biol. Chem. *278*, 48283–48291.

de Jesus, L.A., Carvalho, S.D., Ribeiro, M.O., Schneider, M., Kim, S.W., Harney, J.W., Larsen, P.R., and Bianco, A.C. (2001). The type 2 iodothyronine deiodinase is essential for adaptive thermogenesis in brown adipose tissue. J. Clin. Invest. *108*, 1379–1385.

Dobrzyn, P., Dobrzyn, A., Miyazaki, M., Cohen, P., Asilmaz, E., Hardie, D.G., Friedman, J.M., and Ntambi, J.M. (2004). Stearoyl-CoA deaturase-1 deficiency increases fatty acid oxidation by activating AMP-activated protein kinase in liver. Proc. Natl. Acad. Sci. USA *101*, 6409–6414.

Estabrook, R.W. (1967). Mitochondrial respiratory control and the polarographic measurement of ADP: O ratios. In Methods in Enzymology, Oxidation and Phosphorylation, R.W. Estabrook and M.E. Pullman, eds. (New York: Academic Press), pp. 41–47.

Evans, R.M., Barish, G.D., and Wang, Y.X. (2004). PPARs and the complex journey to obesity. Nat. Med. *10*, 355–361.

Grundy, S.M. (2004). Obesity, metabolic syndrome, and cardiovascular disease. J. Clin. Endocrinol. Metab. *89*, 2595–2600.

Horton, J.D., Shimomura, I., Brown, M.S., Hammer, R.E., Goldstein, J.L., and Shimano, H. (1998). Activation of cholesterol synthesis in preference to fatty acid synthesis in liver and adipose tissue of transgenic mice overproducing sterol regulatory element-binding protein-2. J. Clin. Invest. *101*, 2331–2339.

Jump, D.B., Thelen, A.P., and Mater, M.K. (2001). Functional interaction between sterol regulatory element-binding protein-1c, nuclear factor Y, and 3,5,3′-triiodothyronine nuclear receptors. J. Biol. Chem. *276*, 34419–34427.

Kamei, Y., Ohizumi, H., Fujitani, Y., Nemoto, T., Tanaka, T., Takahashi, N., Kawada, T., Miyoshi, M., Ezaki, O., and Kakizuka, A. (2003). PPARgamma coactivator 1beta/ERR ligand 1 is an ERR protein ligand, whose expression induces a high-energy expenditure and antagonizes obesity. Proc. Natl. Acad. Sci. USA *100*, 12378–12383.

Kopecky, J., Clarke, G., Enerback, S., Spiegelman, B., and Kozak, L.P. (1995). Expression of the mitochondrial uncoupling protein gene from the aP2 gene promoter prevents genetic obesity. J. Clin. Invest. *96*, 2914–2923.

Kopecky, J., Rossmeisl, M., Hodny, Z., Syrovy, I., Horakova, M., and Kolarova, P. (1996). Reduction of dietary obesity in aP2-Ucp transgenic mice: mechanism and adipose tissue morphology. Am. J. Physiol. *270*, E776–E786.

Kuriyama, H., Liang, G., Engelking, L.J., Horton, J.D., Goldstein, J.L., and Brown, M.S. (2005). Compensatory increase in fatty acid synthesis in adipose tissue of mice with conditional deficiency of SCAP in liver. Cell Metab. *1*, 41–51.

Laffitte, B.A., Chao, L.C., Li, J., Walczak, R., Hummasti, S., Joseph, S.B., Castrillo, A., Wilpitz, D.C., Mangelsdorf, D.J., Collins, J.L., et al. (2003). Activation of liver X receptor improves glucose tolerance through coordinate regulation of glucose metabolism in liver and adipose tissue. Proc. Natl. Acad. Sci. USA *100*, 5419–5424.

Li, B., Nolte, L.A., Ju, J.S., Han, D.H., Coleman, T., Holloszy, J.O., and Semenkovich, C.F. (2000). Skeletal muscle respiratory uncoupling prevents diet-induced obesity and insulin resistance in mice. Nat. Med. *6*, 1115–1120.

Liang, G., Yang, J., Horton, J.D., Hammer, R.E., Goldstein, J.L., and Brown, M.S. (2002). Diminished hepatic response to fasting/refeeding and liver X receptor agonists in mice with selective deficiency of sterol regulatory element-binding protein-1c. J. Biol. Chem. *277*, 9520–9528.

Lin, J., Puigserver, P., Donovan, J., Tarr, P.T., and Spiegelman, B.M. (2002). Peroxisome proliferator-activated receptor gamma coactivator 1beta (PGC-1beta), a novel PGC-1-related trancription coactivator associated with host cell factor. J. Biol. Chem. *277*, 1645–1648.

Lin, J., Tarr, P.T., Yang, R., Rhee, J., Puigserver, P., Newgard, C.B., and Spiegelman, B.M. (2003). PGC-1beta in the regulation of hepatic glucose and energy metabolism. J. Biol. Chem. *278*, 30843–30848.

Muscat, G.E., Wagner, B.L., Hou, J., Tangirala, R.K., Bischoff, E.D., Rohde, P., Petrowski, M., Li, J., Shao, G., Macondray, G., and Schulman, I.G. (2002). Regulation of cholesterol homeostasis and lipid metabolism in skeletal muscle by liver X receptors. J. Biol. Chem. *277*, 40722–40728.

Ntambi, J.M., Miyazaki, M., Stoehr, J.P., Lan, H., Kendziorski, C.M., Yandell, B.S., Song, Y., Cohen, P., Friedman, J.M., and Attie, A.D. (2002). Loss of stearoyl-CoA desaturase-1 function protects mice against adiposity. Proc. Natl. Acad. Sci. USA *99*, 11482–11486.

Pachucki, J., Hopkins, J., Peeters, R., Tu, H., Carvalho, S.D., Kaulbach, H., Abel, E.D., Wondisford, F.E., Ingwall, J.S., and Larsen, P.R. (2001). Type 2 iodothyroninedeiodinase transgene expression in the mouse heart causes cardiac-specific thyrotoxicosis. Endocrinology *142*, 13–20.

Peet, D.J., Turley, S.D., Ma, W., Janowski, B.A., Lobaccaro, J.M., Hammer, R.E., and Mangelsdorf, D.J. (1998). Cholesterol and bile acid metabolism are impaired in mice lacking the nuclear oxysterol receptor LXR alpha. Cell *93*, 693–704.

Puigserver, P., and Spiegelman, B.M. (2003). Peroxisome proliferator-activated receptor-gamma coactivator 1 alpha (PGC-1 alpha): transcriptional coactivator and metabolic regulator. Endocr. Rev. *24*, 78–90.

Repa, J.J., and Mangelsdorf, D.J. (2002). The liver X receptor gene team: potential new players in atherosclerosis. Nat. Med. *8*, 1243–1248.

Repa, J.J., Liang, G., Ou, J., Bashmakov, Y., Lobaccaro, J.M., Shimomura, I., Shan, B., Brown, M.S., Goldstein, J.L., and Mangelsdorf, D.J. (2000a). Regulation of mouse sterol regulatory element-binding protein-1c gene (SREBP-1c) by oxysterol receptors, LXRalpha and LXRbeta. Genes Dev. *14*, 2819–2830.

Repa, J.J., Turley, S.D., Lobaccaro, J.A., Medina, J., Li, L., Lustig, K., Shan, B., Heyman, R.A., Dietschy, J.M., and Mangelsdorf, D.J. (2000b). Regulation of absorption and ABC1-mediated efflux of cholesterol by RXR heterodimers. Science *289*, 1524–1529.

Schneider, M.J., Fiering, S.N., Pallud, S.E., Parlow, A.F., St Germain, D.L., and Galton, V.A. (2001). Targeted disruption of the type 2 selenodeiodinase gene (DIO2) results in a phenotype of pituitary resistance to T4. Mol. Endocrinol. *15*, 2137–2148.

Schwarz, M., Russell, D.W., Dietschy, J.M., and Turley, S.D. (1998). Marked reduction in bile acid synthesis in cholesterol 7 alpha-hydroxylase-deficient mice does not lead to diminished tissue cholesterol turnover or to hypercholesterolemia. J. Lipid Res. *39*, 1833–1843.

Tontonoz, P., and Mangelsdorf, D.J. (2003). Liver X receptor signaling pathways in cardiovascular disease. Mol. Endocrinol. *17*, 985–993.

Um, S.H., Frigerio, F., Watanabe, M., Picard, F., Joaquin, M., Sticker, M., Fumagalli, S., Allegrini, P.R., Kozma, S.C., Auwerx, J., and Thomas, G. (2004). Absence of S6K1 protects against age- and diet-induced obesity while enhancing insulin sensitivity. Nature *431*, 200–205.

Wang, Y.X., Lee, C.H., Tiep, S., Yu, R.T., Ham, J., Kang, H., and Evans, R.M. (2003). Peroxisome-proliferator-activated receptor delta activates fat metabolism to prevent obesity. Cell *113*, 159–170.

Yoshikawa, T., Shimano, H., Amemiya-Kudo, M., Yahagi, N., Hasty, A.H., Matsuzaka, T., Okazaki, H., Tamura, Y., Iizuka, Y., Ohashi, K., et al. (2001). Identification of liver X receptor-retinoid X receptor as an activator of the sterol regulatory element-binding protein 1c gene promoter. Mol. Cell. Biol. *21*, 2991–3000.

Yuan, M., Konstantopoulos, N., Lee, J., Hansen, L., Li, Z.W., Karin, M., and Shoelson, S.E. (2001). Reversal of obesity- and diet-induced insulin resistance with salicylates or targeted disruption of Ikkbeta. Science *293*, 1673–1677.

Zhou, Z., Yon Toh, S., Chen, Z., Guo, K., Ng, C.P., Ponniah, S., Lin, S.C., Hong, W., and Li, P. (2003). Cidea-deficient mice have lean phenotype and are resistant to obesity. Nat. Genet. *35*, 49–56.